J. exp. Biol. **140**, 35–49 (1988)
Printed in Great Britain © *The Company of Biologists Limited 1988*

ULTRASTRUCTURE, MORPHOLOGY AND ORGANIZATION OF BIOGENIC MAGNETITE FROM SOCKEYE SALMON, *ONCORHYNCHUS NERKA*: IMPLICATIONS FOR MAGNETORECEPTION

BY STEPHEN MANN, NICHOLAS H. C. SPARKS
School of Chemistry, University of Bath, Bath BA2 7AY, UK

MICHAEL M. WALKER* AND JOSEPH L. KIRSCHVINK
Division of Geological and Planetary Sciences, California Institute of Technology, Pasadena, CA 91125, USA

Accepted 11 May 1988

Summary

Although ferromagnetic material has been detected in the tissues of a variety of animals that are known or suspected to respond to magnetic fields, in only a few cases has the material been identified and its suitability for use in magnetoreception been determined. Using high-resolution transmission electron microscopy (HRTEM), we have studied magnetic particles isolated from ethmoid tissue of the sockeye salmon, *Oncorhynchus nerka*. Low-magnification electron micrographs showed chains containing up to 58 (median = 21–25) electron-dense particles that were held together by intimately attached organic material. The particle size range was 25–60 nm with a mean of 48 nm and a standard deviation of 8·5 nm. Elemental analysis, by energy-dispersive X-ray analysis (EDXA), electron diffraction patterns and HRTEM lattice images, showed that many of the particles were structurally well-ordered and crystallographically single-domain magnetite. These results imply that the production of the biomineral is under precise biological control. The crystal morphology was cubo-octahedral with the {111} faces of adjacent crystals lying perpendicular to the chain axis. The magnetic moments of the particles will therefore be aligned along the chain axis and will sum to produce a total moment dependent on the number of particles present in each chain. In the presence of the geomagnetic field, the mean moment for the particles will give a magnetic to thermal energy ratio of about 0·2. The corresponding calculations for individual chains gave two clusters of ratios ranging between 2·7 and 5·3 and between 6·6 and 9·5. The implications of these results in the possible use of the particles in magnetoreception are discussed.

* Present address: Békésy Laboratory of Neurobiology, University of Hawaii, 1993 East-West Road, Honolulu, HI 96822, USA.

Key words: biogenic magnetite, sockeye salmon (*Oncorhynchus nerka*), magnetoreception, biomineralization.

Introduction

Discovery of the ferrimagnetic mineral, magnetite, first in polyplacophoran molluscs (Lowenstam, 1962) and later in magnetotactic bacteria (Frankel *et al.* 1979) and metazoan species (Gould *et al.* 1978; Walcott *et al.* 1979), provided a plausible mechanism for the hypothesis that animals detect the earth's magnetic field. Theoretical analyses (Yorke, 1979, 1981; Kirschvink & Gould, 1981; Kirschvink & Walker, 1985) showed that magnetite particles used in magnetoreception must have a net magnetic moment sufficient to align themselves with the geomagnetic field against the randomizing effect of thermal buffeting. The best particles for this function are magnetic single-domains, which are uniformly magnetized and have the maximum magnetization per unit volume for magnetite. Such particles can be detected in tissue samples by measuring the coercivity spectrum, that is, the range of applied magnetic fields necessary to magnetize or demagnetize a sample completely. Interacting magnetic single-domains were identified by measurement of coercivity spectra for connective tissue from within the dermethmoid bone of the skull of the yellowfin tuna *Thunnus albacares* (Walker *et al.* 1984) and within the ethmoid cartilage of the skull of the chinook salmon *Oncorhynchus tshawytscha* (Kirschvink *et al.* 1985). Magnetic particles from the ethmoid tissues of the tuna and chinook salmon were uniformly sized, magnetic single-domains of magnetite, some of which were arranged in chains. The uniform size of the magnetite particles in the yellowfin tuna and chinook salmon strongly implied that the particles were produced under close biological control. However, the particles would meet the energetic criterion for use in magnetoreception only if they were arranged in interacting arrays in which the moments of the particles were aligned. It will thus be important to establish that both the particles and the chains are produced under biological control and that the chains are of appropriate length for use in magnetoreception.

A study of different life stages indicated orderly production throughout life of interacting single-domains of magnetite in the front of the skull of the sockeye salmon, *Oncorhynchus nerka* (Walker *et al.* 1988). The sockeye was selected for study because experimental studies have indicated different responses to magnetic field direction in two different life stages, fry and smolts (Quinn, 1980; Quinn & Brannon, 1982). In the experiments reported here, we first used HRTEM and electron microdiffraction to identify magnetite isolated from the ethmoid tissue of adult sockeye salmon. From particle size measurements and HRTEM lattice imaging we then determined the domain state and the degree of structural perfection and crystallographic morphology of individual magnetite crystals. Finally, we investigated the arrangement of the magnetite crystals into chains and their association with organic material in an attempt to elucidate further the possible use of the particles in magnetoreception.

Materials and methods

In the magnetically shielded, dust- and particle-free clean laboratory at the

California Institute of Technology, we extracted magnetic material for mineralogical identification using electron diffraction analysis: we removed the ethmoid tissues of several adult fish, ground them with glass-distilled water in a glass tissue grinder, digested the suspended material in nitrocellulose-filtered (0·45 μm pore size) 5% sodium hypochlorite solution (commercial bleach), and separated released fats by dissolving them in ether. To permit HRTEM analyses, the magnetic particles released by this process were not treated with the cation-chelating agents (EDTA, EGTA) used on magnetic particle extracts from yellowfin tuna and chinook salmon (Walker *et al.* 1984; Kirschvink *et al.* 1985). Instead, they were centrifuged, washed, aggregated magnetically, and resuspended in distilled water (Walker *et al.* 1985), and then posted in a sealed container to the University of Bath, England.

At Bath, the suspension was allowed to stand for 24 h next to the north pole of a bar magnet. The resulting aggregate was removed with the aid of a glass Pasteur pipette and resuspended ultrasonically in 1 cm^3 of Analar-grade chloroform. Drops of the suspension were air dried on carbon-coated, nitrocellulose-covered, copper electron microscope grids and investigated using a JEOL 100 CX analytical transmission electron microscope and a JEOL 2000 FX high-resolution transmission electron microscope fitted with a Link AN 10000 energy-dispersive X-ray analysis facility. Lattice images were recorded at 200 keV with an objective aperture of 80 μm and a point-to-point resolution capable of 2·8 Å (1 Å = 0·1 nm).

Transmission electron micrographs of the crystals were analysed to provide crystal measurements. 104 discrete crystals were measured at 0° tilt angle. The numbers of particles in 18 crystal chains, which were selected using two criteria, were measured. First, only isolated chains with a significant number of crystals (>12) were measured, as smaller chains may represent chain fragmentation induced by sample preparation procedures. Second, areas of chain folding and particle clumping were rejected and only straight lengths of continuous intact chain were measured. A magnetic moment was calculated for the mean particle size, whereas moments for the chains were calculated by summing the mean particle moment for all the particles within each chain. These estimates were more conservative than those based on the summation of individual moments calculated for each particle in the chain.

Results

Low-magnification electron micrographs of the extracted magnetic material from the ethmoid tissue of sockeye salmon showed chains of electron-dense particles associated with granular organic material (Fig. 1). No distinct cellular components could be identified. Although many chains were continuous, others were significantly disrupted, presumably because of the sonication and drying procedures employed during sample preparation. Still other chains appeared to be folded on themselves or attached end to end and looped around other chains. The tendency to clump at these points may be explained by the magnetic field patterns

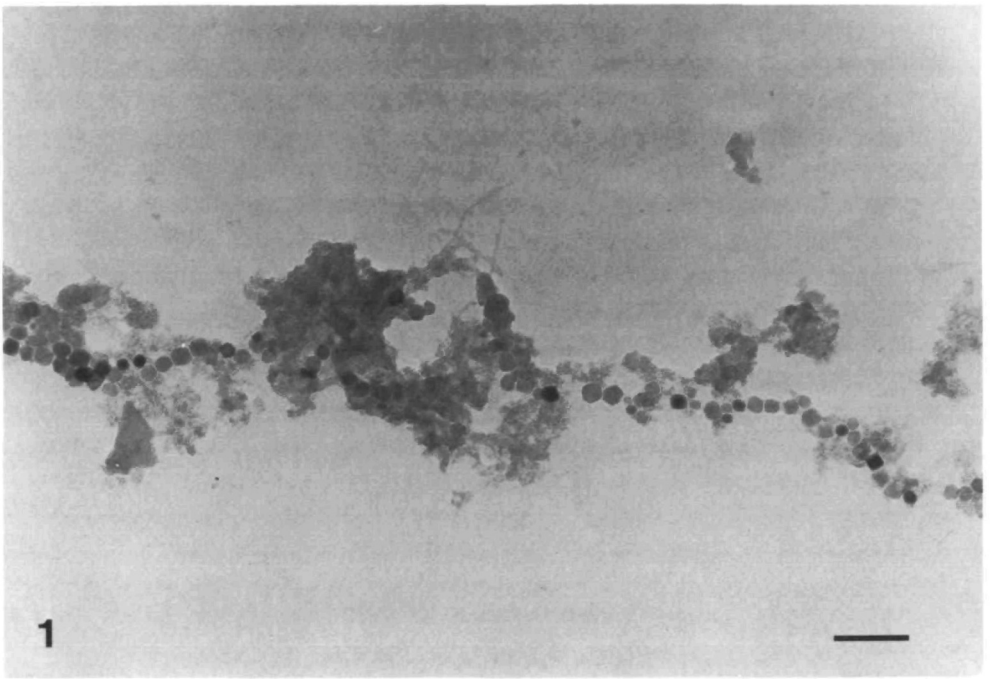

Fig. 1. Magnetic extract from the ethmoid tissue of sockeye salmon showing a chain of electron-dense particles associated with organic material. Scale bar, 200 nm.

surrounding elongated chains. Numerical calculation of these patterns has demonstrated that most of the high field and gradients are focused at the ends of the chains (J. L. Kirschvink, in preparation). As a result of the clumping in the chains isolated from the sockeye, the number of crystals per chain was difficult to measure. Chains meeting the criteria for measurement of the number of particles they contained varied in length (Fig. 2). Most contained between 13 and 45

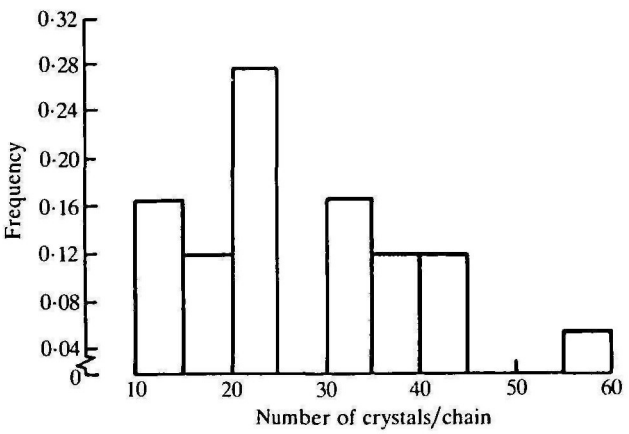

Fig. 2. Distribution of the number of particles per intact chain.

particles and fell into separate length groups with modal values of 21–25 and 35–40 particles. The one chain not in these two groups contained 58 particles. The median chain length fell in the 21–25 particle length class (Fig. 2). The particle size range was 25–60 nm with a mean of 48 nm and a standard deviation of 8·5 nm (Fig. 3). Particles at both extremes of the size range showed a morphology characteristic of isotropic faceted crystals viewed in projection (Fig. 4).

Although tissue debris was associated with the chains, much of this was non-specific. Crystals that were located in areas relatively free from contamination, however, clearly showed the presence of intimately attached organic material which appeared to link the particles within a viscous gel, thereby providing structural integrity to the individual chains (Fig. 5). Elemental analysis of individual particles by EDXA showed Fe as the only inorganic constituent (elements below atomic number = 10 could not be detected by this technique; Fig. 6). Crystallographic determination of the particles was undertaken using electron microdiffraction and HRTEM. d-spacings calculated from diffraction patterns were consistent with the mineral, magnetite (Fe_3O_4; Table 1). In addition, electron microdiffraction patterns showed that individual particles were crystallographically single-domain crystals (Fig. 7). These results were confirmed by HRTEM images of individual crystals which showed lattice fringes, with interplanar spacings and angular relationships consistent with the magnetite space group, traversing the total extent of the particles (Fig. 8). The structural perfection of the single-domain crystallites was high, as shown by the continuous and periodic nature of the lattice fringes. In particular, the crystal edges were often well-defined and no amorphous or structural irregularities such as edge dislocations were observed. The orientation of the {111} lattice planes shown in Fig. 8 indicates that the well-developed edges of the crystals correspond to the octahedral {111} faces. In addition, the regularity of the {111} planes at the crystal edges implies that these faces are often atomically smooth. Other micrographs (data not shown) indicated that the small truncated faces were of the form {100} which, together

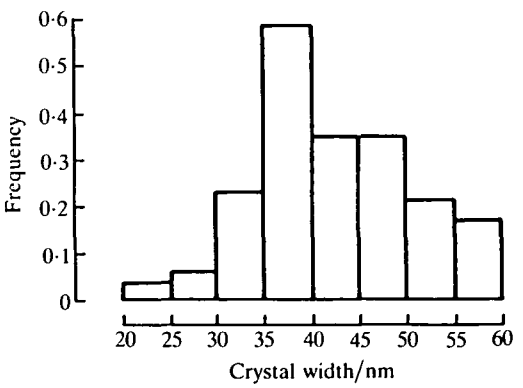

Fig. 3. Size frequency distribution of magnetic crystals.

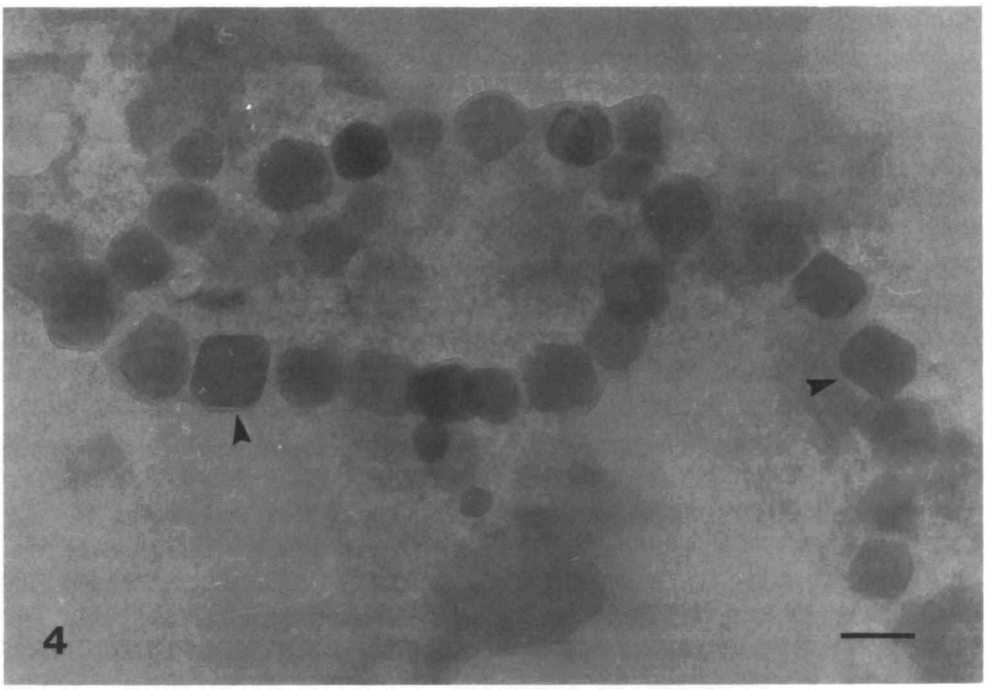

Fig. 4. Chain of magnetic crystals showing characteristic truncated octahedral morphologies (arrowheads). Scale bar, 50 nm.

with the above data, is consistent with a crystal morphology based on a cubo-octahedral habit.

Magnetite crystals within individual chains exhibited a preferred crystallographic orientation with the {111} faces of adjacent crystals lying perpendicular to the chain direction. This observation was not only apparent in low-magnification electron micrographs (Fig. 4) but also in lattice images recorded on adjacent crystals (Fig. 9). In these images, the {111} planes of neighbouring crystals were in almost total alignment, even though the crystals were not contiguous because of a thin organic interface.

A few particles showed lattice images consistent with twinned magnetite crystals (Fig. 10). Most of these particles were single (contact) twins with the twin plane centrally located within the two-domain crystals. Fig. 10 shows a lattice image of a twinned crystal with each domain showing a different set of lattice planes ({111} and {200}) which intersect along the central dark line (the twin boundary). The angle between the lattice planes at the domain interface is 165°. This value is consistent with the theoretically calculated value for a magnetite crystal oriented along the [011] crystallographic direction and corresponds to the angle between the (200) plane, twinned along a $(11\bar{1})$ reflection plane, and the $(1\bar{1}1)$ plane of the parent crystal. Also, $(1\bar{1}1)$ planes are coincident across the $(11\bar{1})$ reflection plane. Note that the presence of these crystal twin planes does not necessarily imply the

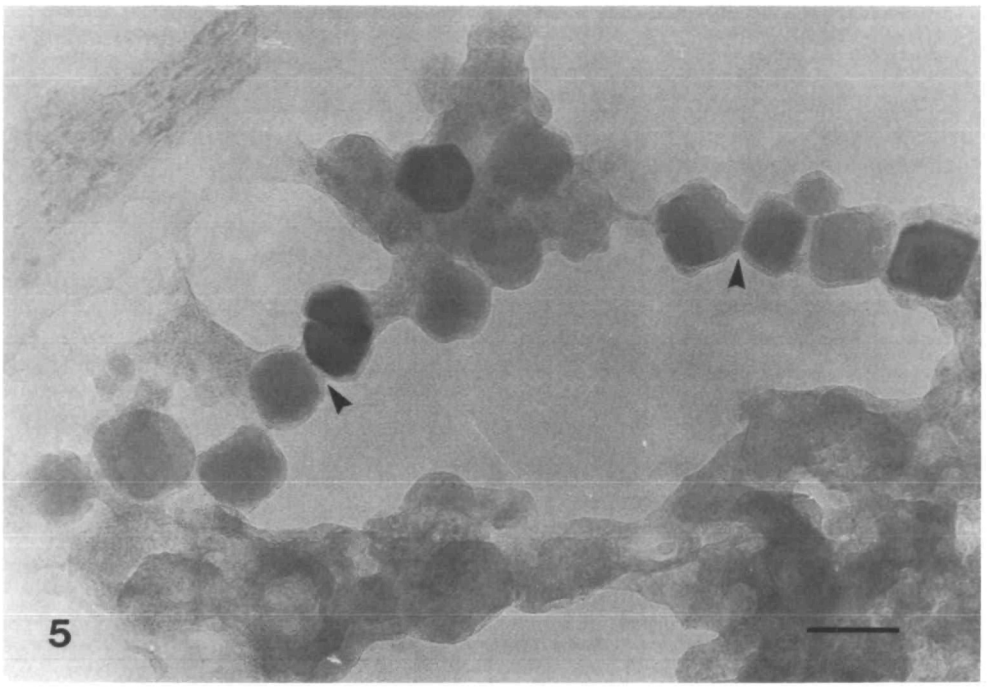

Fig. 5. Chain of magnetic crystals showing organic material intimately associated with, and interlinking, the particles (arrowheads). Scale bar, 50 nm.

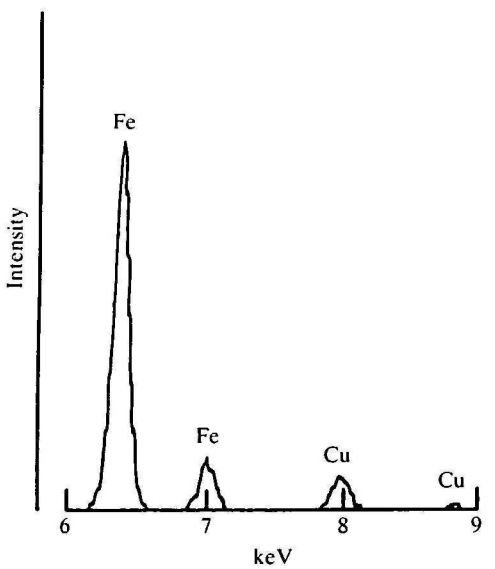

Fig. 6. Energy dispersive spectrum from an individual magnetic particle.

Table 1. *Electron diffraction data for crystals extracted from ethmoid tissue of sockeye salmon*

Electron diffraction pattern (powder)		
Sockeye (Å)	Magnetite (Å)*	(hkl)
4·20	4·20	(200)
2·59	2·532	(311)
2·03	2·099	(400)
1·75	1·715	(422)
1·42	1·419	(531)
1·28	1·281	(533)
1·12	1·122	(642)
1·05	1·050	(800)
0·85	0·856	(844)

* ASTM card 19–629.

presence of a magnetic domain wall boundary; the electronic superstructure, and hence transfer of super-exchange coupled electrons, are continuous across the junction and should allow the entire particle to be magnetically single-domain.

The moments (μ) of the 104 particles measured in Fig. 3 were estimated from the relationship:

$$\mu = \mathrm{VJs},$$

where V is the volume of each crystal and Js is the saturation magnetization for magnetite ($4{\cdot}8\times10^{5}\,\mathrm{A\,m^{-1}}$). Although only two crystal dimensions could be measured from the electron micrographs, comparison of crystals in different orientations implied that the particles were roughly equant in shape. The volume of each particle was calculated on the basis of an octahedral crystal morphology as inferred from the HRTEM results. The calculated moments varied with variation in the estimates of particle volume and had a mean magnetic to thermal energy ratio of about 0·2. The preferred crystallographic orientation, with the {111} faces of adjacent crystals lying perpendicular to the chain direction, constrains the moments of the individual particles to lie in the axis of the chain. The moments of the particles in individual chains therefore sum to give interaction energies (μB) with the 50 μT (0·5 Gauss) geomagnetic field spanning a range of values with respect to the background thermal energy (kT) (Fig. 11).

Discussion

The electron diffraction and electron microscopy data presented in this paper clearly show that the magnetic material extracted from the ethmoid tissue of adult sockeye salmon is in the form of individual chains of magnetite crystals. The possibility that the formation of chains is artefactual, arising from magnetic aggregation during sample preparation, can be ruled out for two reasons. First, the

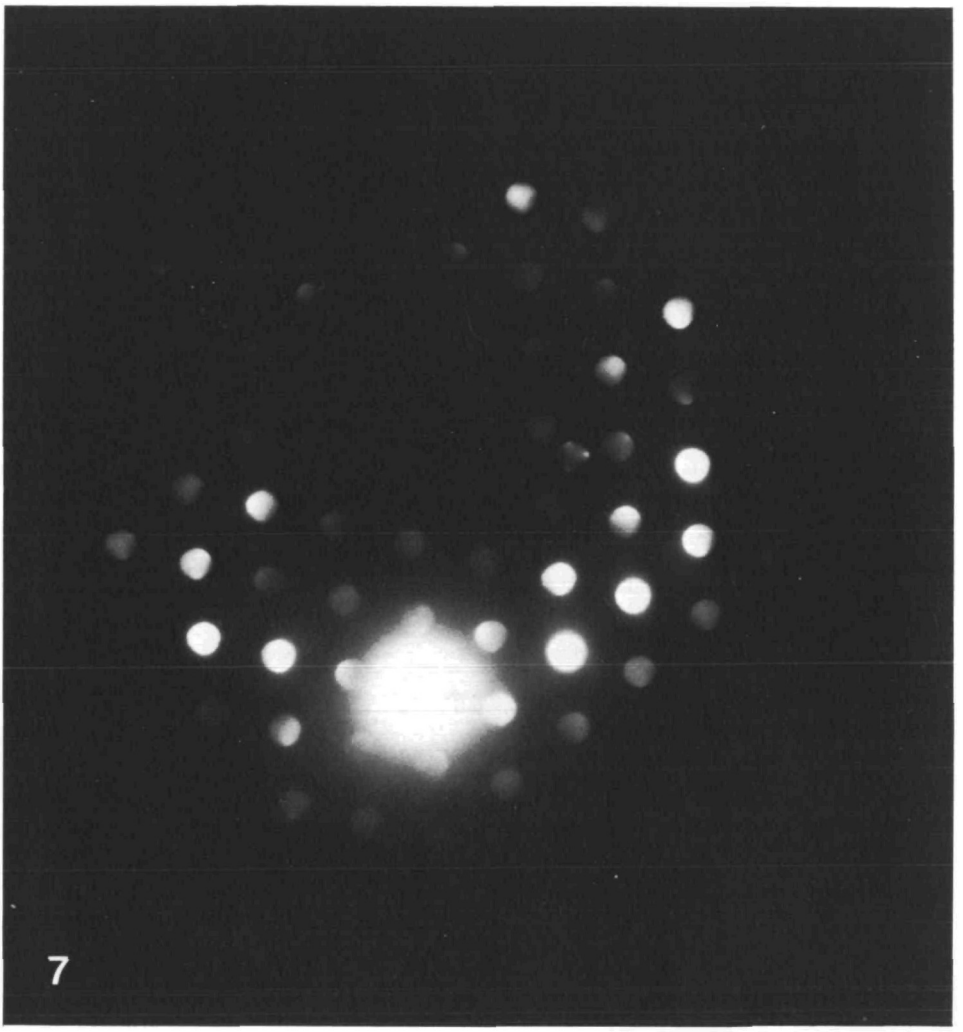

Fig. 7. Electron microdiffraction pattern from an individual magnetic particle. The pattern corresponds to the ⟨110⟩ zone of magnetite (Fe_3O_4). Camera length, 180 cm.

crystals are intimately associated with organic material which restricts the magnetic alignment of individual particles in a dispersed sample. Second, previous experience with both bacterial and inorganic magnetites has shown minimal evidence for magnetic alignment when the samples have been prepared as described in this paper. The crystals are, in general, structurally well-ordered and crystallographically single-domain. The particle size distribution and morphology are restricted such that the crystals lie within the boundaries established for magnetically single-domain magnetite (Butler & Banerjee, 1975). These results confirm the interpretation that magnetic coercivity data previously obtained for this species are consistent with single-domain magnetite (Walker *et al.* 1988). The

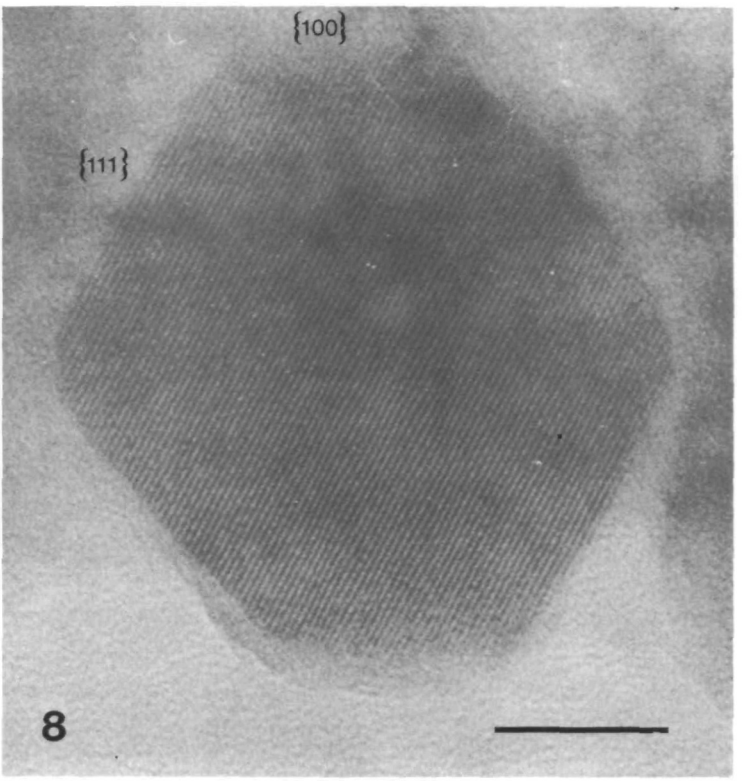

Fig. 8. Lattice image of an individual magnetite crystal showing well-ordered {111} (4·85 Å) fringes. Note the well-defined {111} edges. The smaller truncated faces are of {100} form seen in approximate ⟨110⟩ projection. The crystals have characteristic cubo-octahedral morphologies. Scale bar, 10 nm.

results also indicate that, although both structural and magnetic properties need to be determined for detailed characterization of biomagnetic deposits, coercivity data are generally reliable in cases where the amount of material is exceedingly low and difficult to isolate for structural studies; for example, in early life stages such as smolts, yearlings and newly hatched fry.

The presence within the ethmoid tissue of magnetite crystals with well-defined structure, morphology, size and crystallographic orientation within an organic matrix implies that this biomineral develops within or in close association with cells under precise biological control. The adoption of a cubo-octahedral morphology, which is also characteristic of abiogenic magnetites, suggests that the growth of the biological crystals is essentially thermodynamically governed and not subject to extensive kinetic and surface-specific mediation as is the case in some bacterial magnetites (Mann *et al.* 1984*b*, 1987). In the case of the sockeye salmon and the magnetotactic bacterium *Aquaspirillum magnetotacticum*, the alignment of the {111} faces perpendicular to the chain axis is probably a function of the effect of crystal growth in the high magnetic field at the end of a chain (J. L.

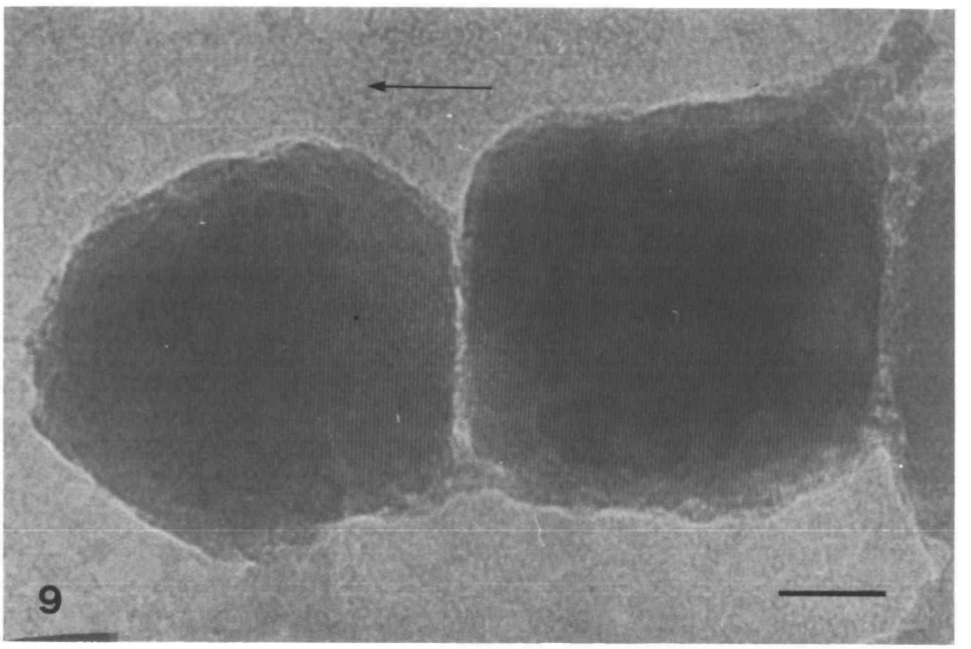

Fig. 9. Lattice images of two adjacent magnetite crystals showing the preferential crystallographic orientation of both crystals such that the {111} lattice planes lie perpendicular to the chain axis (arrow). Scale bar, 10 nm.

Kirschvink, in preparation) rather than the result of epitaxial template control. The {111} axis is the preferred direction of magnetization for magnetite and this alignment of the axes of a newly growing magnetite particle represents the minimum-energy configuration. In many respects, the crystallochemical aspects of the sockeye salmon magnetite is similar to that found in *Aquaspirillum magnetotacticum* (Mann *et al.* 1984*a*), except that the chain lengths in the salmon tissue are significantly greater. We feel that this morphological similarity justifies the use of the descriptive term 'magnetosome' for the crystals in salmon, as these structures possess all major features of the bacterial organelles used in its initial definition by Balkwill *et al.* (1980).

Although it is not possible to determine chain length with certainty, our results are consistent with the use of the chains in magnetoreception. It is uncertain whether the frequency distribution of numbers of particles in the chains represents multiple length classes or integral multiples of a single chain length class. Potential sources of variation in chain length include chain fragmentation due to the tissue digestion and sonication used to separate the chains before mounting, joining of chains as a result of incomplete separation by the sonication procedure, and chain reaggregation in the drying stage of mounting. The optimal numbers of particles required for use of the chains to monitor magnetic field intensity and direction are about 10 and 30 particles, respectively (Kirschvink & Walker, 1985). Fig. 11 shows that the $\mu B\,kT^{-1}$ values fall within two clusters, between 2·7 and 5·3 and between

6·6 and 9·5, consistent with the hypothesis that both intensity and direction cues could be used in magnetoreception in sockeye salmon. Furthermore, this result suggests that the control of the size and shape of the individual magnetite particles and of the length of the chains in which they are arranged has arisen as a result of

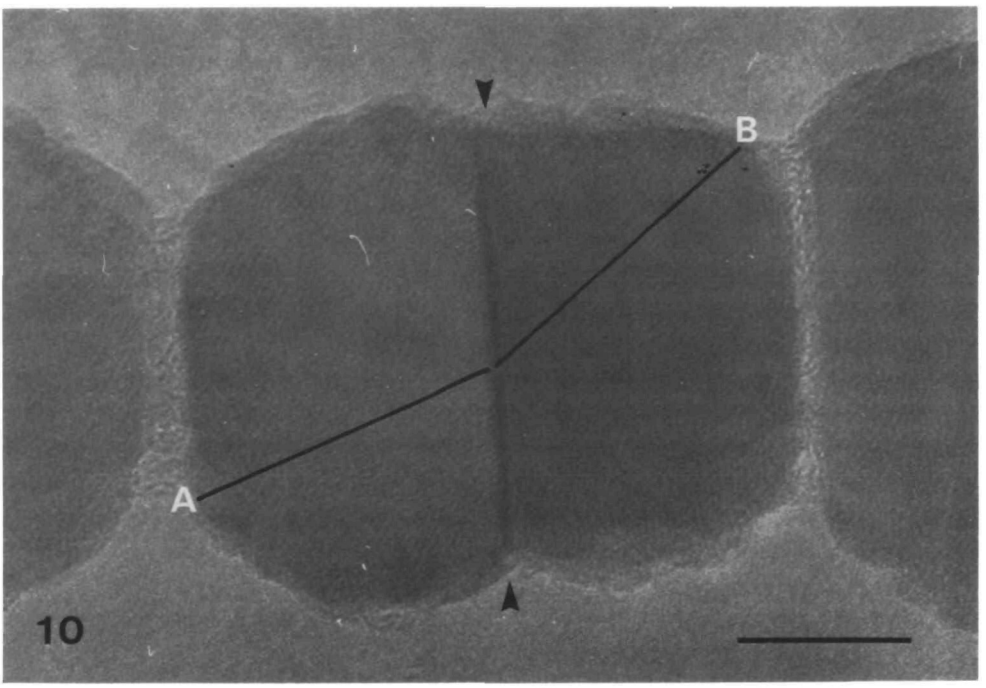

Fig. 10. Magnetite crystal twinned along a (11$\bar{1}$) reflection plane (arrowheads). The crystal is viewed down the [011] axis such that the angle between the (1$\bar{1}$1) (A) and twinned (200) (B) planes is 165°. (The fringes are more clearly seen by viewing the micrograph almost parallel to the plane of the page.) Scale bar, 10 nm.

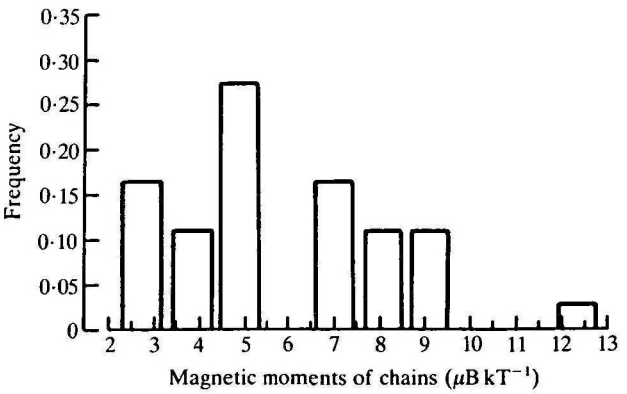

Fig. 11. Distribution of magnetic moment/thermal energy ratios for individual chains of magnetite crystals isolated from sockeye salmon.

selection for their magnetic properties. The single long chain at 12·3 μB kT^{-1} may be a composite of several smaller chains.

The procedures used here for extraction of biogenic magnetite and in a companion study (Walker *et al.* 1988) for distinguishing single-domain and multidomain material in tissue samples present new opportunities for the comparative study of magnetite produced by organisms. First, the organic material surrounding the magnetite particles extracted from the sockeye salmon resembles the matrix that holds together the magnetosome in the magnetotactic bacteria (Balkwill *et al.* 1980) and presumably also in the magnetotactic algae (Torres de Araujo *et al.* 1986). Fossilized magnetosomes have now been detected in sedimentary rocks dating at least to the early proterozoic (≈2 billion years ago; Chang, 1987; Chang *et al.* 1987) which is 400 million years prior to the first record of eukaryotes. This observation raises the possibility that magnetite production in the bacteria and metazoans has a common origin. Testing antibodies to the bacterial magnetosomes for activity against the organic material surrounding the magnetite particles in the salmon could potentially provide a powerful test of this hypothesis as well as a useful probe for histological demonstration of the particles in the intact tissue. Even if such a test were not possible, it should be possible to investigate the role of the attached organic material in the formation of the magnetite particles and chains extracted from the salmon using the same techniques as have been used to investigate magnetite formation in the bacteria (e.g. see Balkwill *et al.* 1980; Frankel *et al.* 1985).

The second area for further work involves biologically precipitated magnetic material other than the single-domain magnetite investigated so far. In our studies of magnetic material in tissues of the sockeye salmon and other pelagic fishes, we have detected magnetically soft, multidomain particles of unknown composition (Walker *et al.*1988; Kirschvink *et al.* 1985). In addition, coarse-grained material has been found in TEM studies of magnetic particles extracted from magnetic tissue samples from a variety of species (Hanson *et al.* 1984; Perry *et al.* 1985; Walker *et al.* 1985; S.-B. R. Chang, unpublished data; S. Mann & N. H. C. Sparks, unpublished data). Such deposits have not yet been studied in detail. Because the tissue from the ethmoid region of the skull has been the only reliably magnetic tissue we have found, both within and among species of pelagic fishes, it has been difficult to establish whether deposits of coarse-grained material were contaminants entering during dissection and extraction procedures or were true biological precipitates. Although a biological origin for coarse-grained deposits would suggest a wider range of uses for biogenic magnetite than simple magnetoreception, it would also provide indirect evidence that single-domain particles and the chains in which they occur have been selected for because of their magnetic properties.

We thank Drs T. P. Quinn and C. Groot of the Pacific Biological Station (Department of Fisheries and Oceans, Nanaimo, British Columbia, V9R 5K6, Canada) for supplying the adult sockeye salmon heads. This research was

supported by SERC grants GR/D/62243 and GR/D/30754; NSF grants BNS 83-00301, PYI-8351370; BRSG funding from NIH; and grants from the Weyerhauser Corporation and the Keck Foundation. Contribution no. 4551 from the Division of Geological and Planetary Sciences, California Institute of Technology, Pasadena CA 91125, USA.

References

BALKWILL, D. L., MARATEA, D. & BLAKEMORE, R. P. (1980). Ultrastructure of a magnetotactic spirillum. *J. Bacteriol.* **141**, 1399–1408.

BUTLER, R. F. & BANERJEE, S. K. (1975). Theoretical single-domain size in magnetite and titanomagnetite. *J. geophys. Res.* **80**, 4049–4058.

CHANG, S.-B. R. (1987). Bacterial magnetite in sedimentary deposits and its geophysical and paleoecological implications. Ph.D. thesis, California Institute of Technology, Pasadena, California. 266pp.

CHANG, S.-B. R., KIRSCHVINK, J. L. & STOLZ, J. F. (1987). Biogenic magnetite as a primary remanence carrier in limestone deposits. *Phys. Earth plan. Int.* **46**, 289–303.

FRANKEL, R. B., BLAKEMORE, R. P. & WOLFE, R. S. (1979). Magnetite in freshwater magnetotactic bacteria. *Science* **203**, 1355–1356.

FRANKEL, R. B., PAPAEFTHYMIOU, G. C. & BLAKEMORE, R. P. (1985). Mössbauer spectroscopy of iron biomineralization products in magnetotactic bacteria. In *Magnetite Biomineralization and Magnetoreception in Organisms: A New Biomagnetism* (ed. J. L. Kirschvink, D. S. Jones & B. J. MacFadden), pp. 269–287. New York, London: Plenum Press.

GOULD, J. L., KIRSCHVINK, J. L. & DEFFEYES, K. S. (1978). Bees have magnetic remanence. *Science* **201**, 1026–1028.

HANSON, M., WIRMARK, G., OBLAD, M. & STRID, L. (1984). Iron-rich particles in European eel (*Anguilla anguilla* L.). *Comp. Biochem. Physiol.* **79**A, 311–316.

KIRSCHVINK, J. L. & GOULD, J. L. (1981). Biogenic magnetite as a basis for magnetic field detection in animals. *Biosystems* **13**, 181–201.

KIRSCHVINK, J. L. & WALKER, M. M. (1985). Particle-size considerations for magnetite-based magnetoreceptors. In *Magnetite Biomineralization and Magnetoreception in Organisms: A New Biomagnetism* (ed. J. L. Kirschvink, D. S. Jones & B. J. MacFadden), pp. 243–254. New York, London: Plenum Press.

KIRSCHVINK, J. L., WALKER, M. M., CHANG, S.-B., DIZON, A. E. & PETERSON, K. A. (1985). Chains of single-domain magnetite particles in chinook salmon, *Oncorhynchus tshawytscha*. *J. comp. Physiol.* **157**, 375–381.

LOWENSTAM, H. A. (1962). Magnetite in denticle capping in recent chitons (Polyplacophora). *Geol. Soc. Am. Bull.* **73**, 435–438.

MANN, S., FRANKEL, R. B. & BLAKEMORE, R. P. (1984*a*). Structure, morphology and growth of bacterial magnetite. *Nature, Lond.* **310**, 405–407.

MANN, S., MOENCH, T. T. & WILLIAMS, R. J. P. (1984*b*). A high resolution electron microscopic investigation of bacterial magnetite. Implications for crystal growth. *Proc. R. Soc.* B **221**, 385–393.

MANN, S., SPARKS, N. H. C. & BLAKEMORE, R. P. (1987). Structure, morphology and crystal growth of anisotropic magnetite crystals in magnetotactic bacteria. *Proc. R. Soc.* B **231**, 477–487.

PERRY, A., BAUER, G. B. & DIZON, A. E. (1985). Magnetoreception and biomineralization of magnetite in amphibians and reptiles. In *Magnetite Biomineralization and Magnetoreception in Organisms: A New Biomagnetism* (ed. J. L. Kirschvink, D. S. Jones & B. J. MacFadden), pp. 439–453. New York, London: Plenum Press.

QUINN, T. P. (1980). Evidence for celestial and magnetic compass orientation in lake-migrating sockeye salmon fry. *J. comp. Physiol.* **137**, 243–248.

QUINN, T. P. & BRANNON, E. L. (1982). The use of celestial and magnetic cues by orienting sockeye salmon smolts. *J. comp. Physiol.* **147**, 547–552.

TORRES DE ARAUJO, F. F., PIRES, M. A., FRANKEL, R. B. & BICUDO, C. E. M. (1986). Magnetite and magnetotaxis in algae. *Biophys. J.* **50**, 375–378.

WALCOTT, C., GOULD, J. L. & KIRSCHVINK, J. L. (1979). Pigeons have magnets. *Science* **205**, 1027–1029.

WALKER, M. M., KIRSCHVINK, J. L., CHANG, S.-B. R. & DIZON, A. E. (1984). A candidate magnetic sense organ in the yellowfin tuna, *Thunnus albacares*. *Science* **224**, 751–753.

WALKER, M. M., KIRSCHVINK, J. L., PERRY, A. & DIZON, A. E. (1985). Detection, extraction, and characterization of biogenic magnetite. In *Magnetite Biomineralization and Magnetoreception in Organisms: A New Biomagnetism* (ed. J. L. Kirschvink, D. S. Jones & B. J. MacFadden), pp. 155–166. New York, London: Plenum Press.

WALKER, M. M., QUINN, T. P., KIRSCHVINK, J. L. & GROOT, C. (1988). Production of single-domain magnetite throughout life by sockeye salmon *Oncorhynchus nerka*. *J. exp. Biol.* **140**, 51–63.

YORKE, E. D. (1979). A possible magnetic transducer in birds. *J. theor. Biol.* **77**, 101–105.

YORKE, E. D. (1981). Sensitivity of pigeons to small magnetic field variations. *J. theor. Biol.* **89**, 533–537.